Journal of Dentistry 54 (2016) 33–40

Contents lists available at ScienceDirect

Journal of Dentistry

journal homepage: www.intl.elsevierhealth.com/journals/jden

Effects of surface properties of polymer-based restorative materials on early adhesion of *Streptococcus mutans in vitro*

Chongyang Yuan[a], Xiaoyan Wang[a,*], Xuejun Gao[a], Feng Chen[b], Xinjie Liang[c], Dehui Li[c]

[a] Department of Cariology and Endodontology, Peking University School and Hospital of Stomatology, Beijing 100081, China
[b] Department of Central Laboratory, Peking University School and Hospital of Stomatology, Beijing 100081, China
[c] Research and Development Department, Advanced Technology & Materials Corporation Ltd., Beijing 100094, China

ARTICLE INFO

Article history:
Received 23 March 2016
Received in revised form 13 July 2016
Accepted 20 July 2016

Keywords:
Polymer-based restorative materials
Bacterial adhesion
Surface properties
Confocal laser scanning microscopy

ABSTRACT

Objective: We investigated the effects of the surface properties of polymer-based restorative materials on early adhesion of *Streptococcus mutans* (UA159) *in vitro*.
Methods: Four direct polymer-based restorative materials, including a nanoparticle restorative (Filtek™ Z350, 3 M ESPE, USA), a nano hybrid universal restorative (Filtek™ Z250 XT, 3 M ESPE, USA), a low shrink posterior restorative (Filtek™ P90, 3 M ESPE, USA) and a polymer-based pre-reacted glass ionomer (Beautifil II, Shofu, Japan), were selected. After polishing under different conditions, surface morphology was examined using scanning electron microscopy. Surface roughness (SR), water contact angle (CAW) and surface free energy (SFE) were determined by profilometry and the sessile drop method. Early adhesion of *S. mutans* was investigated using confocal laser scanning microscopy. The area occupied by adherent bacteria (A%) was calculated with COMSTAT2 software. The correlations between A% and SR, CAW, and SFE were analyzed by linear regression using SPSS 20.0 software at a significance level of 0.05.
Results: The value of A% was strongly correlated with SR ($r = 0.893$, $P < 0.01$) for surface roughness (Ra) of 0.02–0.80 μm, whereas a weaker correlation was obtained between A% and SR when Ra ≤ 0.20 μm ($r = 0.643$, $P < 0.01$). On super smooth surfaces (0.02 μm ≤ Ra ≤ 0.06 μm), SR did not influence early bacterial adhesion ($r = 0.001$, $P > 0.05$), a medium positive correlation between A% and SFE was obtained ($r = 0.426$, $P < 0.01$), and no correlation between A% and CAW was found ($r = -0.028$, $P > 0.05$)
Conclusions: Early adhesion of *S. mutans* on direct polymer-based restorative materials was mainly affected by SR. SFE influenced early adhesion of *S. mutans* on super smooth surfaces, while hydrophobicity did not.

1. Introduction

Dental plaque or biofilms are the main causes of common dental diseases, and involve microbial adhesion to dental hard and soft tissues as well as restorative biomaterials [1,2]. The mechanisms whereby oral bacteria adhere to solid surfaces are influenced by the unique adhesive properties of the adherent bacteria as well as the properties of the adhered substances. Secondary caries development is closely related to the presence of cariogenic biofilms on dental restorative materials [3]. Previous studies have reported that the three-dimensional structure and thickness of dental biofilms, as well as the composition and activity of dental plaque influenced by restorative materials [4,5]. In addition to the different compositions of diverse substances, the surface properties of restorative materials play a pivotal role in the early adhesion process of bacteria [6,7].

Polymer-based dental composites are an aesthetic alternative to amalgam, and are composed of a hydrophobic resin matrix containing hydrophilic filler particles, which implies they form a heterogeneous surface. The polymer composition, and the size and shape of fillers strongly influence the surface properties of polymer-based composites [8,9]. In recent years, to improve the mechanical, physical, and biological properties of polymer-based composites, a multitude of modified polymer-based restorative materials have been developed. For example, an innovative matrix-modified resin composite based on siloxane and oxirane [10] was developed to decrease polymerization shrinkage. The resulting siloranes exhibit similar or better mechanical and physical properties and biocompatibility characteristics than those of conventional methacrylate-based composite resins [11–14]. Regarding development of inorganic fillers, nanofilled resin composites exhibit excellent hardness, toughness, and polishing

* Corresponding author.
E-mail address: wangxiaoyan@pkuss.bjmu.edu.cn (X. Wang).

http://dx.doi.org/10.1016/j.jdent.2016.07.010
0300-5712/

characteristics. Meanwhile, pre-reacted glass-ionomer (PRG) bioactive fillers have been fabricated by the acid–base reaction between a fluoroaluminosilicate glass and polyalkenoic acid in the presence of water [15]. The addition of bioactive fillers results in fluoride releasing/recharging properties to prevent secondary caries [16]. These modified polymer-based composites possessing varied surface properties may influence bacterial adhesion differently.

Oral bacterial adhesion occurs in the following four phases [17,18]: (1) transport of a bacterium to the surface, (2) initial adhesion with reversible and irreversible stages, (3) attachment by specific interactions, and (4) colonization to form a biofilm. Non-specific chemical and electrovalent interactions between the surface and bacteria, like Van der Waals forces, Coulomb forces, and hydrophobic, electrostatic and Lewis acid–base interactions, affect this process [2]. The physicochemical surface properties of restorative materials, such as their surface roughness (SR), hydrophobicity, surface free energy (SFE), and surface electrochemistry, may affect dental plaque formation [5,18]. It has been reported that SR is the dominant factor influencing bacterial adhesion [17,18]. An increase in SR from 0.2 to 0.8 μm of intraoral hard surfaces had a significant effect on *in vivo* plaque formation (supra- and subgingivally) on abutments [19]. Therefore, a threshold surface roughness (Ra) was suggested. When $Ra \leq 0.2$ μm, it was considered that SR had a negligible effect on bacterial adhesion *in vivo* [20]. However, with the development of polymer-based materials and polishing technology, the bacterial adhesion on polished materials below the threshold value of Ra has varied considerably [21]. This indicates that when $Ra \leq 0.2$ μm, factors other than SR influence bacterial adhesion.

It has been observed that SFE and hydrophobicity also affect bacterial adhesion on polymer-based materials [21–24]. However, the published results are quite controversial [10,25–32]. Possible reasons for these controversial results may be the heterogeneous composition of polymer-based composite surfaces, and the methods used to evaluate SFE and hydrophobicity. It has been reported that the SFE and hydrophobicity (contact angle of water, CAW) values calculated with the sessile drop method is more accurate when the surface is smoother [33,34]. Therefore, the effects of SFE and CAW on bacterial adhesion should be interpreted with caution. Furthermore, it has been considered that the effects of SFE and CAW on bacterial adhesion may be confounded by the dominant role of SR, especially when Ra is above 0.06 μm [34–36]. Therefore, it remains unclear if the SFE and/or hydrophobicity of polymer-based composite materials influence bacterial adhesion, especially on smooth surfaces.

In this study, the SR, CAW, and SFE of polymer-based restorative materials, along with early adhesion of *Streptococcus mutans* on them are investigated. The correlations between these factors are analyzed. The aim of this study is to gain more insight into the surface properties responsible for initial adhesion of *S. mutans* on polymer-based restorative materials. We hypothesize that the levels of early adhesion of *S. mutans* are influenced not only by SR, but also by hydrophobicity and SFE, especially on smooth surfaces.

2. Materials and methods

2.1. Preparation of polymer-based restorative material specimens

Four polymer-based restorative materials were used in this study, including a nanoparticle restorative (Filtek™ Z350 [Z350], 3M ESPE, USA), a nano-hybrid universal restorative (Filtek™ Z250 XT [Z250 XT], 3 M ESPE, USA), a low-shrink posterior restorative based on siloxane and oxirane (Filtek™ P90 [P90], 3 M ESPE, USA) and a polymer-based pre-reacted glass ionomer (Beautifil II [BF], Shofu, Japan). The parameters of these materials are summarized in Table 1. Each polymer-based material was placed in a fabricated Teflon model ($4 \times 4 \times 2$ mm) and covered with a Mylar film. A glass slide was placed over the Mylar film, and pressure was applied. After curing under high-intensity light (1100 mW/cm^2) on both sides for 40 s (LEDition, Ivoclar vivadent), all specimens were stored in distilled water at 37 °C for 24 h, and then polished with a polisher (AutoMet® 250 Grinder-Polisher Family, Buehler, USA). A continuous force of 5 N in the vertical direction rotation speed of 60 rpm/150 rpm at contrary motion was applied. The specimens were sequentially polished with 11-μm grit (grain 1200 wet abrasive paper disc, White Dove, China), 9-μm grit, 3-μm grit, 1-μm disc (diamond disc, Lapping Film ϕ250 mm, Grish, China), and finally nano-silicon dioxide fabric (Polishing Pad S0-PGZ-2 ϕ250 mm, GRISH, China). After polishing, specimens were rinsed with distilled water and ultrasonically cleaned in distilled water for 3 min. According to the final polishing grit, the specimens were divided into five groups for each material: Group 1: 11-μm grit; Group 2: 9-μm grit; Group 3: 3-μm grit; Group 4: 1-μm grit; Group 5: nano grit.

2.2. Surface morphology

The surface morphology of specimens was examined with a scanning electron microscope (SEM, S-4800, Hitachi, Japan). After mounting on aluminum stubs and sputter coating with gold, the specimens were observed with 1000× magnification.

Table 1
Resin-based restorative materials used in the study.

Type	Brand name	Matrix composition	Filler composition	Manufacturer
Nanoparticle composite	Filtek™ Z350 [Z350]	Bis-GMA, Bis-EMA, UDMA, TEGDMA	5–20 nm non-agglomerated silica and 5–20 nm zirconium/silica nanoagglomerate. 0.6-1.4 μm agglomerated particles. Loading percentage by weight: 82%	3M ESPE, St. Paul, MN, USA
Nano hybrid composite	Filtek™ Z250 XT [Z250 XT]	Bis-GMA, Bis-EMA, UDMA, TEGDMA, PEGDMA	20 nm surface modified silica and 0.1–10 μm surface modified zirconia/silica particles. Loading percentage by weight: 82%	3M ESPE, St. Paul, MN, USA
Silorane composite	Filtek™ P90 [P90]	Bis-3,4-epoxy cyclohexylethyl phenyl methyl silane-, 3,4-epoxy cyclohexyl cyclopolymethyl siloxane, di- and epoxy-functional oligosiloxane	trifluoride ITRE, 0.1–2 μm quartz particles. Loading percentage by weight: 76%	3M ESPE, St. Paul, MN, USA
Giomer	Beautifil II [BF]	Bis-GMA, TEGDMA	0.01–4.0 μm multi-functional glass filler and S-PRG filler based on fluoroboroaluminosilicate glass. Loading percentage by weight: 81%	Shofu Inc., Japan

Bis-GMA, bisphenol A-glycidyl dimethacrylate; UDMA, urethane dimethacrylate; Bis-EMA, bisphenol A ethoxylate dimethacrylate; TEGDMA, triethyleneglycol dimethacrylate; PEGDMA, polyethyleneglycol dimethacrylate; S-PRG, surface pre-reacted glass ionomer.

2.3. Surface roughness measurement

The SR of each specimen was measured using a surface profilometer (Surftest SJ-401, Mitutoyo, Kanagawa, Japan) with a stress force of 0.75 mN, standard cutoff of 1.0 mm, transverse length of 0.8 mm, amplitude height of 2.5 μm, and stylus speed of 0.5 mm/s. Two measurements of Ra were performed at cross directions for each specimen, and the numerical average of these values is reported.

2.4. Hydrophobicity and surface free energy determination

Hydrophobicity was determined by measuring the water contact angles with an automated contact angle measurement device (OCA20, DataPhysics, Germany). Right and left contact angles for droplets (1 μL) were averaged and are reported as CAW (°).

To determine the SFE of each specimen, three liquids with different polarities were chosen for contact angle measurements, including distilled water, glycerol, and ethylene glycol. The SFE of each specimen is listed in Table 2 [37]. The total SFE (γ^{TOT}) for each sample was calculated according to the approach proposed by van Oss et al.:

$$\gamma_S^{TOT}(mN/m) = \gamma_S^D + \gamma_S^P;$$

$$\gamma_S^P = 2\left(\gamma_S^+\gamma_S^-\right)^{0.5};$$

$$(1+\cos\theta)\gamma_L^{TOT} = 2\left(\gamma_S^D\gamma_L^D\right)^{0.5} + 2\left(\gamma_L^-\gamma_S^+\right)^{0.5} + 2\left(\gamma_L^+\gamma_S^-\right)^{0.5}.$$

2.5. Bacteria preparation and adhesion experiments

The serotype c strain *Streptococcus mutans* UA 159 was obtained from the Institute of Microbiology, Chinese Academy of Sciences. The frozen (−80 °C) precultured bacteria were transferred onto an agar plate with brain heart infusion broth (BHI; BD, Becton, Dickinson and Company, USA) and incubated at 37 °C in 95% air/5% CO_2 (*v/v*) for 48 h. Subsequently, a single colony was incubated with sterile BHI under the same conditions for 16 h and then kept at 4 °C. The day before the experiment, *S. mutans* suspension (1 mL) was added to fresh sterile BHI (250 mL) and incubated for 12 h at 37 °C. After harvesting by centrifugation (2200 rpm, 19 °C, 5 min; Centrifuge 5418, Eppendorf, Germany), bacteria cells were washed twice with phosphate-buffered saline (PBS; one packet dissolved in deionized water (2 L), pH 7.4 at 25 °C; Solarbio, China) and then resuspended in the PBS. The optical density of the bacterial suspension was adjusted with PBS to 0.3 at 550 nm (EL × 808 Absorbance Microplate Reader, Bio-Tek, USA), which corresponds to a microbial concentration of 3.65×10^8 cells/mL [38].

Before adhesion, all material specimens were sterilized by degassing with ethylene oxide for more than 48 h, transferred into a sterile 24-well plate, and then incubated with *S. mutans* suspension (1 mL) in a thermo shaker (THZ-22, Tcsysb, China) at a speed of 60 rpm at 37 °C. After 2.5 h, the specimens were gently rinsed twice with PBS to remove unbound bacteria, and then analyzed by confocal laser scanning microscopy (CLSM).

Table 2
Testing liquids and surface tension data ($mN \cdot m^{-1}$).

Liquid	Surface tension data ($mN \cdot m^{-1}$)			
	γ_L^{TOT}	γ_L^D	γ_L^+	γ_L^-
Glycerol	64	34	3.92	57.4
Ethylene glycol	48	29	3	30.1
Distilled water	72.8	21.8	25.5	25.5

γ_L^{TOT}, total surface free energy; γ_L^D, dispersive component; γ_L^+, Lewis-acid component; γ_L^-, Lewis-base component.

2.6. Confocal laser scanning microscopy analysis

One volume of BacLight stain contains SYTO 9 and propidium iodide (LIVE/DEAD® BacLight™ Bacteria Viability Kit, L-7012, Invitrogen Inc., USA). The excitation/emission maxima of these two dyes are approximately 480/500 nm for SYTO 9 and 490/635 nm for propidium iodide, respectively. Live bacteria were stained with SYTO 9 to produce green fluorescence. Bacteria with compromised membranes were stained with propidium iodide to produce red fluorescence.

Following staining in the dark for 15 min at room temperature, all specimens were rinsed gently with distilled water twice, subjected to CLSM (Zeiss LSM 510, Carl Zeiss Microscopy, Jena, Germany), and examined with argon (514/488 nm) and HeNe (543 nm) lasers. Nine squares of the surface were divided equally, and bacteria adhesion at the central portion of each square with 450× magnification (size: 102.11 × 102.11 μm) was analyzed. The area occupied by the bacteria on the surface of each specimen was calculated using COMSTAT2 software (http://www.comstat.dk for free) and recorded as A%. The median value of A% for each specimen was calculated further.

2.7. Statistical analysis

The medians and 25%–75% quartiles of Ra and A% were determined and statistically analyzed using nonparametric tests/independent-samples tests/Mann-Whitney *U* tests at a significance level of 0.05 (SPSS 20.0, IBM, USA). The mean and standard deviation of CAW and γ^{TOT} were determined and statistically analyzed using one-way ANOVA tests (LSD/Dunnett T3) with *P* value of 0.05. Correlations between A% and Ra, CAW, and γ^{TOT} were analyzed using linear regression, and are presented in corresponding equations and scatter plots.

3. Results

3.1. Surface morphology

The typical surface morphology of the specimens is shown in Fig. 1. All the polymer-based materials possessed a heterogeneous surface composed of inorganic fillers and organic resin matrix. For all materials, the surfaces contained fewer scratches from Group 1 to Group 5. Group 1 and Group 2 samples contained a large number of scratches, whereas almost no scratches were present on the surfaces of materials in Group 3, Group 4 and Group 5, for which the fillers were distinguishable.

3.2. Surface roughness, hydrophobicity, and surface free energy

The values of SR (Ra), hydrophobicity (CAW) and SFE (γ^{TOT}) of the materials are presented in Table 3. For all materials, Group 1 showed the highest Ra (median 0.43∼0.67 μm). As polishing progressed, Ra decreased, and then became constant. Ra of surfaces in Group 3, Group 4, and Group 5 were similar (median 0.02∼0.03 μm), and much lower than those of Group 1 and Group 2 (median 0.09∼0.16 μm). Although P90 and Z250 XT showed higher Ra than Z350 and BF in Group 1 and Group 2, all four materials presented similar Ra in Group 3, Group 4, and Group 5.

Considering hydrophobicity, all the polymer-based materials presented decreased CAW as polished progressed ($P < 0.05$). Among the four materials, P90 showed a higher CAW and was

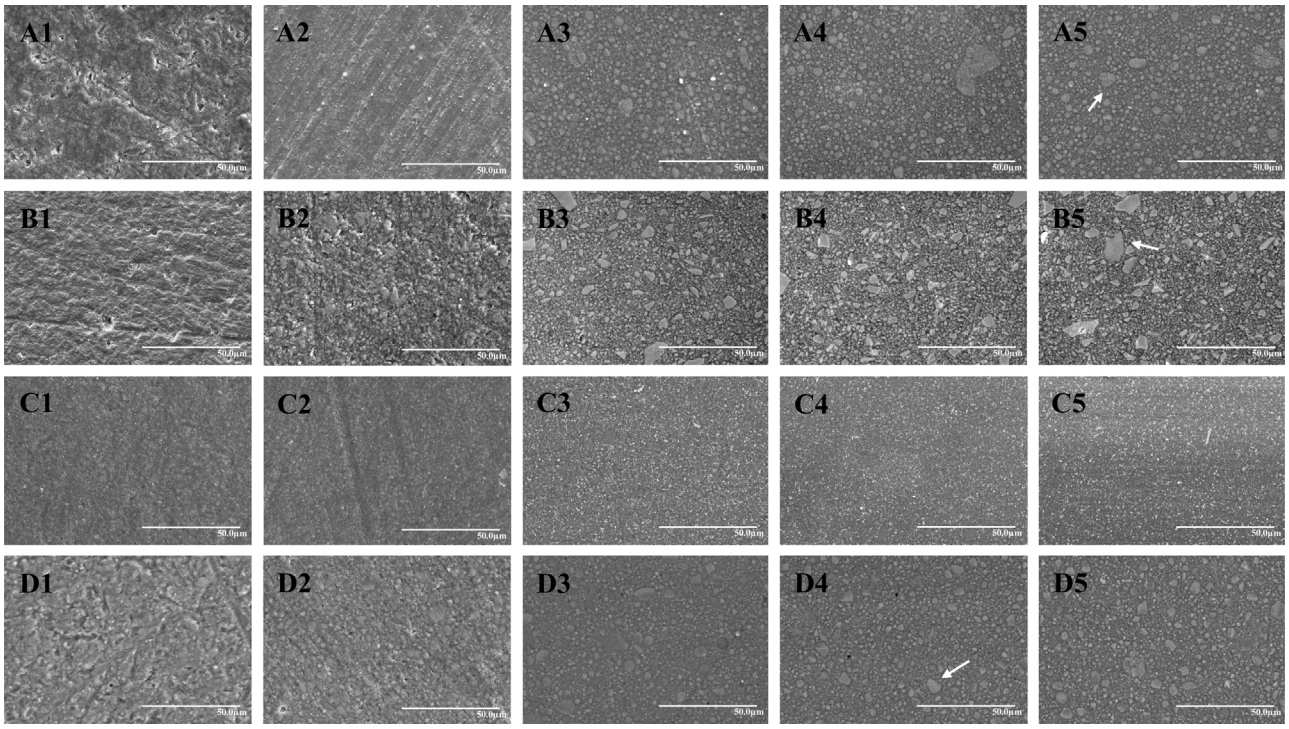

Fig. 1. SEM showing the surface morphology of materials before bacteria adhesion (×1000). A, B, C and D represent the Filtek™ Z350, Beautifil II, Filtek™ P90 and Filtek™ Z250, respectively. 1, 2, 3, 5 and 5 represent polishing Group1, Group2, Group 3, Group 4 and Group 5, respectively. The arrows shown in image A5, B5 and D4 indicate fillers on the polished surfaces.

Table 3
Surface roughness (Median (25/75%), water contact angle and surface free energy (Mean ± SD).

	Materials	Group1	Group2	Group3	Group4	Group5
Surface roughness (Ra/μm)	Filtek™Z350	0.44 (0.39/0.47)$^{a\#}$	0.09 (0.09/0.10)$^{b\#}$	0.02 (0.02/0.02)$^{c\#}$	0.02 (0.02/0.02)$^{c\#}$	0.02 (0.02/0.02)$^{c\#}$
	Beautifil II	0.43 (0.41/0.48)$^{a\#}$	0.13 (0.12/0.14)$^{b\wedge}$	0.03 (0.03/0.04)$^{c\wedge}$	0.03 (0.03/0.03)$^{c\wedge}$	0.02 (0.02/0.03)$^{d\wedge *}$
	Filtek™ P90	0.53 (0.49/0.56)$^{a\wedge}$	0.16 (0.15/0.17)^{b*}	0.03 (0.03/0.04)$^{c\wedge}$	0.03 (0.02/0.03)$^{d\wedge}$	0.02 (0.02/0.02)$^{e\#\wedge}$
	Filtek™Z250 XT	0.67 (0.63/0.74)^{a*}	0.15 (0.14/0.15)$^{b\&}$	0.03 (0.03/0.04)$^{c\wedge}$	0.03 (0.03/0.03)$^{d\wedge}$	0.03 (0.03/0.03)^{d*}
Water contact angle (CAW/°)	Filtek™Z350	83.20 ± 3.20$^{a\#\wedge}$	77.00 ± 4.70$^{b\#\wedge *}$	66.72 ± 2.71$^{c\#}$	62.92 ± 1.24$^{d\#}$	63.78 ± 1.32$^{d\#}$
	Beautifil II	81.44 ± 2.21$^{a\#}$	76.29 ± 1.76$^{b\#}$	71.62 ± 1.64$^{c\wedge}$	65.53 ± 1.68$^{d\wedge}$	65.86 ± 3.67$^{d\#}$
	Filtek™P90	84.26 ± 2.00$^{a\wedge}$	79.58 ± 1.36$^{b\wedge}$	75.04 ± 1.06^{c*}	70.96 ± 1.09^{d*}	69.95 ± 1.52$^{d\wedge}$
	Filtek™Z250 XT	82.42 ± 2.00$^{a\#\wedge}$	72.83 ± 1.51^{b*}	68.41 ± 1.36$^{c\#}$	63.72 ± 1.19$^{d\#}$	59.00 ± 1.74^{e*}
Surface free energy (γ^{TOT}/mN m^{-1})	Filtek™Z350	94.56 ± 16.96$^{a\#}$	76.49 ± 2.81$^{b\#*}$	28.81 ± 2.53$^{c\#}$	80.64 ± 9.64$^{ab\#}$	47.40 ± 9.35$^{d\#}$
	Beautifil II	95.15 ± 11.41$^{a\#}$	54.18 ± 4.79$^{b\wedge}$	43.53 ± 1.61$^{c\wedge}$	36.71 ± 3.29$^{d\wedge}$	66.28 ± 4.97$^{e\wedge}$
	Filtek™P90	67.35 ± 4.34$^{a\wedge}$	51.60 ± 4.04$^{bd\#\wedge}$	47.97 ± 4.43^{b*}	35.75 ± 2.11$^{c\wedge}$	52.69 ± 2.98$^{d\#}$
	Filtek™Z250 XT	90.43 ± 2.85$^{a\#}$	69.44 ± 3.38^{b*}	44.14 ± 1.63$^{c\wedge *}$	82.95 ± 1.34$^{d\#}$	70.64 ± 7.80$^{b\wedge}$

a, b, c, d, e different letters indicate significant differences in surface roughness/water contact angle/surface free energy for the same materials ($P < 0.05$), #, ^, *, & different letters differ among materials in the same group ($P < 0.05$).

more hydrophobic than the other materials, especially in Group 3, Group 4, and Group 5 ($P < 0.05$).

Regarding SFE, all the materials displayed the same trend (Table 3). As polishing progressed, γ^{TOT} decreased at first, and then fluctuated. However, there were significant differences among the lowest SFE value of the samples ($P < 0.05$): Z350 (28.81 mN/m) < BF (36.71 mN/m), P90 (35.75 mN/m) < Z250 XT (40.14 mN/m).

3.3. Bacterial adhesion

S. mutans adhesion on the material surfaces is presented in Fig. 2a. For each material, Group 1 showed the highest amount of bacterial adhesion on each surface. Group 2 showed a lower amount of adhered bacteria than Group 1, but a higher amount of adhered bacteria than those of Group 3, Group 4, and Group 5. The lowest amount of adhered bacteria was observed in Group 4 for BF and P90, Group 3 for Z350, and Group 5 for Z250 XT (Fig. 2b).

For Group 1, similar amounts of bacteria adhered to all the specimens, independent of the type of material. However, for the other groups, the quantity of adhered bacteria varied between the different materials in the same polishing group. P90 and Z350 showed the lowest amounts of adhered bacteria in Group 2 and Group 3 respectively. Conversely, in both Group 4 and Group 5, BF was more resistant to bacterial adhesion than the other materials.

3.3.1. Dependence of bacterial adhesion on the surface roughness of materials

A correlation analysis between the Ra values and A% is shown in Fig. 3. A high linear correlation coefficient ($r = 0.893$, $r^2 = 0.797$)

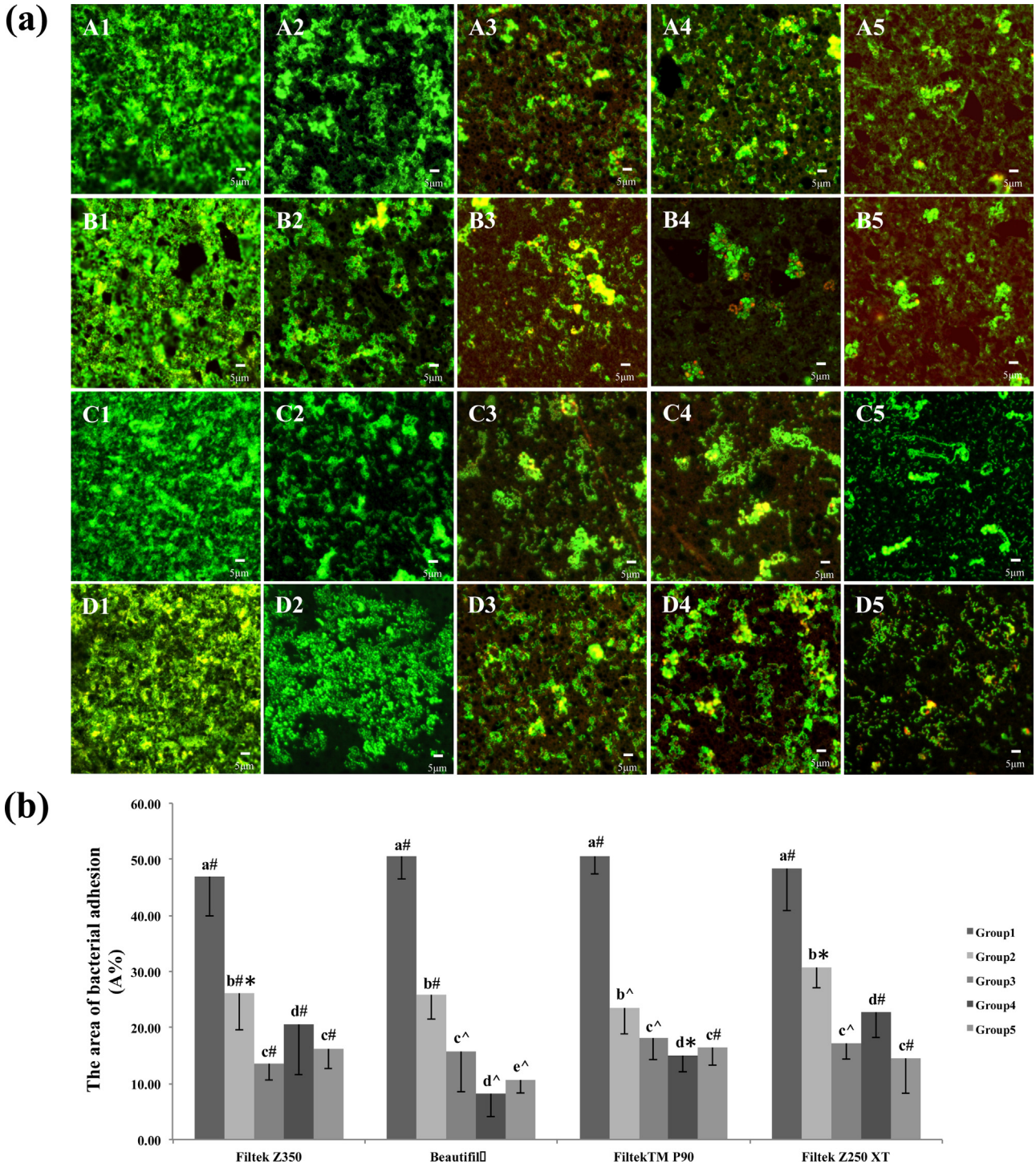

Fig. 2. Bacteria adhesion. (a) CLSM images (× 63/oil/1.4) for bacteria that adhered on materials according to the polishing groups. A, B, C and D represent Filtek™ Z350, Beautifil II, Filtek™ P90 and Filtek™ Z250, respectively. 1, 2, 3, 4 and 5 represent polishing Group 1, Group 2, Group 3, Group 4 and Group 5, respectively. (b) The area of bacteria adhesion (A%). Median and IQR are indicated. Different letters of a, b, c, d, e indicate significant differences for the same materials ($P < 0.05$). Different letters of #, ^, * differ among materials in the same group ($P < 0.05$).

($P < 0.01$) between A% and Ra values was revealed for all specimens regardless of material type. When Ra was lower than the threshold value related to bacterial adhesion of 0.20 μm [20], the correlation between A% and Ra was lowered ($r = 0.643$, $r^2 = 0.414$) ($P < 0.01$). However, for super smooth surfaces (Ra ≤ 0.06 μm) [39,40], there was no correlation between A% and Ra ($r = 0.001$, $r^2 = 0.000$) ($P > 0.05$). This indicates that bacterial adhesion on super smooth surfaces was probably influenced by other factors in addition to SR.

3.3.2. Bacterial adhesion on super smooth surfaces (Ra ≤ 0.06 μm)

A simple scatterplot of A% on super smooth surfaces with Ra ≤ 0.06 μm is depicted in Fig. 4a. Although on similar super smooth surfaces, a distribution of A% was observed, which indicates that some other factors besides Ra influence bacterial adhesion on super smooth surfaces. As shown in Fig. 4b, the correlation between A% and γ^{TOT} on super smooth surfaces was linear. These two variables were positively correlated, as indicated

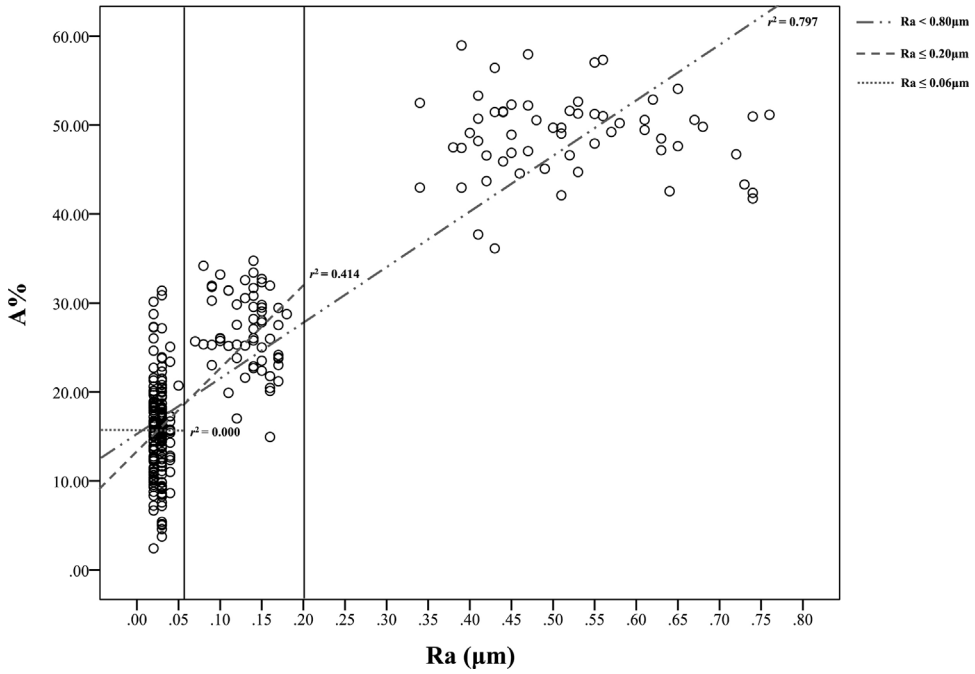

Fig. 3. Correlation analysis between the surface roughness (Ra) and area of bacteria adhesion (A%). When Ra < 0.80 μm, correlations between the Ra and A% on the material surfaces shown as a linear regression line (y = 15.391 + 62.104x) with corresponding 95% confidence limits; correlation coefficient $r = 0.893$, $r^2 = 0.797$; $P < 0.01$. When Ra ≤ 0.20 μm, correlations between the Ra and A% on the material surfaces shown as a linear regression line (y = 13.518 + 92.285x) with corresponding 95% confidence limits; correlation coefficient $r = 0.643$, $r^2 = 0.414$; $P < 0.01$. When Ra ≤ 0.06 μm, there was no correlations between the Ra and A% on the material surfaces with corresponding 95% confidence limits; correlation coefficient $r = 0.001$, $r^2 = 0.000$; $P > 0.05$.

by their positive slope. However, the correlation coefficient ($r = 0.426$, $r^2 = 0.182$) ($P < 0.01$) of this plot was relatively low. The correlation of CAW with A% on super smooth surfaces is illustrated in Fig. 4c. There was no correlation between bacterial adhesion A% and CAW on super smooth surfaces ($r = -0.028$, $r^2 = 0.001$) ($P > 0.05$).

4. Discussion

Our results showed that the SR of polymer-based restorative materials played a major role in the early adhesion of *S. mutans*. SFE was correlated with early bacterial adhesion on super smooth surfaces, while hydrophobicity was not. Therefore, the hypothesis was partially accepted. The polymer-based materials presented a wide range of SR (Ra of 0.02~0.68 μm) after polishing under different conditions. The surface morphology of the specimens indicated that the smaller the polishing abrasive was, the fewer scratches present on the surface, as supported by a previous study [41]. When the surfaces were polished until they were super smooth (Ra ≤ 0.06 μm), no scratches were observed, and the surface morphology was characterized by the size, shape, hardness, quantity, and distribution of filler particles [42–45]. A strong correlation between Ra and A% was observed for all materials. An increase in SR of polymer-based materials resulted in early adhesion of more bacteria, consistent with previous findings [17,46,47]. According to Bollen and co-workers, when Ra ≤ 0.20 μm, SR had a negligible effect on bacteria adherence [19,20,47]. In these previous studies, however, most dental polymer-based materials were relatively smooth after polishing (Ra of 0.1~0.2 μm). In the present study, because of the nano-technique applied in dental polymer-based materials, as well as the improvement of polishing techniques, polymer-based material surfaces can be super smooth after polishing, even mirror-like (Ra ≤ 0.02 μm). Our results showed that there was no significant correlation between SR and A% on the resin composite materials only when Ra ≤ 0.06 μm. When Ra was between 0.06 and 0.2 μm, SR still positively affected early bacterial adhesion. This was also verified by Burgers et al. [36]. However, in this study, we observed that the different polymer-based materials with Ra ≤ 0.06 μm showed different bacterial adhesion. This indicates that some other factor instead of SR played a dominant role in bacterial adhesion on super smooth surfaces (Ra ≤ 0.06 μm).

Two other important surface parameters, SFE and hydrophobicity, are usually determined by contact angle measurement. Although the polymer-based composite was heterogeneous, the fillers distributed uniformly and the particle size was only 0.1–100 μm. Therefore, the test droplet diameter (3.0 mm) was sufficient to cover the uniformly distributed filler–matrix structure, so reliable SFE and CAW data were obtained. However, it has been reported that SR may influence contact angle measurements [40], especially when Ra > 0.1 μm [34]. In addition, because of the dominant role of SR in bacterial adhesion, the effects of SFE and hydrophobicity on bacterial adhesion may be obscured and interpreted inaccurately when Ra > 0.1 μm. Therefore, the influences of SFE and hydrophobicity on early bacterial adhesion were investigated after eliminating the effect of SR by using Ra ≤ 0.06 μm.

The SFE of all four polymer-based materials with super smooth surfaces fluctuated, which was consistent with other studies [42,48]. It has been reported that SFE depends on the filler composition of resin composites [35]. The different fluctuations of SFE observed for the four materials are probably a result of their different filler compositions. The filler in Z350 and Z250 XT is silica and zirconia particles, while those of P90 and BF are quartz and fluoroboroaluminosilicate particles, respectively. It was presumed previously that surface polishing not only removed resin matrix and exposed fillers but also possibly formed a resin smear layer on the polished surface. However, our SEM images did not show any resin smear layers. Future studies should consider the factors related to the fluctuation of SFE on super smooth surfaces. Based on

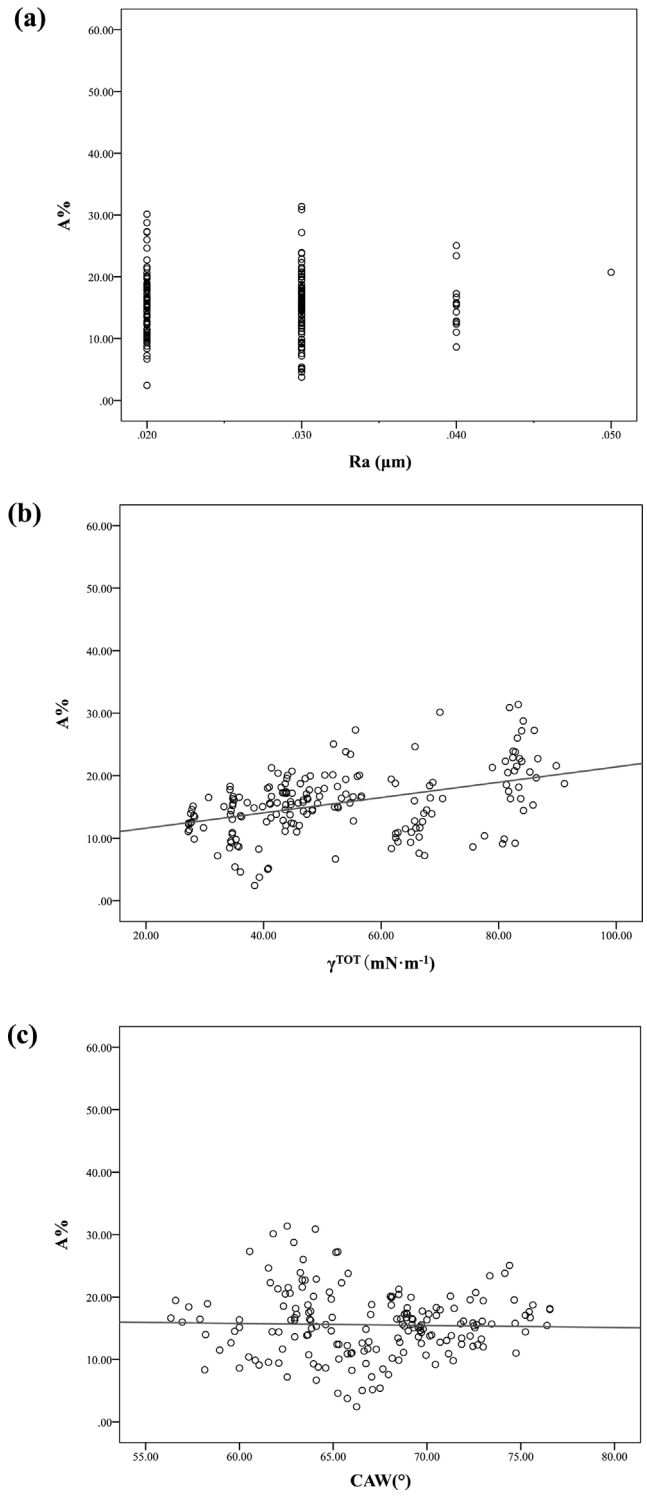

Fig. 4. Bacteria adhesion on super smooth surfaces (Ra ≤ 0.06 μm). (a) Simple scatterplot between A% and Ra. (b) Correlations between the γ^{TOT} and A% shown as a linear regression line (y = 9.031 + 0.125x) with corresponding 95% confidence limits; correlation coefficient $r = 0.426$, $r^2 = 0.182$; $P < 0.01$. (c) There was no correlations between the CAW and A% with corresponding 95% confidence limits; correlation coefficient $r = -0.028$, $r^2 = 0.001$; $P > 0.05$.

the thermodynamic phenomenon [17,18], strains with high SFE (*e.g.*, *S. mutans*) adhered preferentially to substrates with high SFE. In this study, a positive correlation between γ^{TOT} and A% was observed for super smooth surfaces.

It was reported that hydrophilic surfaces have a higher affinity for water-soluble oral bacteria than hydrophobic ones [10,25,26]. However, it has also been reported that increased hydrophobicity of surfaces promotes removal of water between water-soluble bacteria and surfaces, enabling a closer interaction and stronger adhesion forces [27–29]. Thus, the effect of surface hydrophobicity on bacterial adhesion remains quite controversial. These contrasting results may be caused by the different bacteria strains and models used. In addition, the bacterial adhesion periods should be considered. The surface properties of restorative materials influence bacterial adherence but not plaque maturation [49,50], so an adhesion time of 2.5 h was selected in this study. Under the present short-term conditions, the bacterial adhesion strength to surfaces with different hydrophobicity depends on electrostatic forces. According to electrostatic forces, *S. mutans* should tend to bind to hydrophobic surfaces. Although *S. mutans* can rapidly bind to hydrophobic surfaces, the adhesion strength of *S. mutans* to hydrophobic surfaces is weaker than that to hydrophilic surfaces, which could allow bacteria to detach easily from hydrophobic surfaces [51]. The present findings did not provide any evidence that hydrophobicity influenced early bacterial adhesion, especially on smooth surfaces [52]. This was also verified by previous studies finding that there was no significant correlation between the hydrophobicity of polymer-based materials and early bacterial adhesion, at least within 5 h [30–32]. The possible reason for the lack of correlation between hydrophobicity and bacterial adhesion may be that all four materials in this study possessed CAW higher than 62°, so were all hydrophobic surfaces [53].

In addition, some studies found that the bacterial adhesion process varied between materials, depending on their composition [6,17,18,54]. In this study, relatively lower bacterial adhesion was observed on the BF surfaces, which may be a result of it containing antibacterial fluoroboroaluminosilicate particles. Therefore, further investigation of the antibacterial composition of materials and bacterial adhesion is required.

This study provided insight into the correlations between the surface properties and adhesion of *S. mutans*, especially regarding SFE and hydrophobicity on smooth surfaces. However, the bacteria species and acquired pellicle coatings could also affect bacterial adhesion to substrates [44,55–58]. Further studies should investigate how the modification of surfaces affects bacterial adhesion.

5. Conclusions

The correlations between the surface properties (SR, hydrophobicity and SFE) of resin-base restorative materials and *S. mutans* adhesion without saliva coatings were investigated. Within the limitations of this study, *S. mutans* adhesion on the surfaces of polymer-based restorative materials was mainly affected by SR. SFE influenced early bacterial adhesion on the four polymer-based restorative materials with super smooth surfaces, while hydrophobicity did not.

Acknowledgements

This work was supported by grant Z141100000514016 from Beijing Municipal Science & Technology Commission Project (X. Wang). We express our gratitude for the technical assistance (OCA, SEM and EDS) of Institute of Microbiology Chinese Academy of Sciences. In addition, we would like to thank the COMSTAT homepage at http://www.comstat.dk for supporting COMSTAT2 for free.

References

[1] H.J. Busscher, M. Rinastiti, W. Siswomihardjo, H.C. van der Mei, Biofilm formation on dental restorative and implant materials, J. Dent. Res. 89 (7) (2010) 657–665.
[2] C. Hannig, M. Hannig, The oral cavity—a key system to understand substratum-dependent bioadhesion on solid surfaces in man, Clin. Oral Invest. 13 (2) (2009) 123–139.
[3] V. Deligeorgi, I.A. Mjor, N.H. Wilson, An overview of reasons for the placement and replacement of restorations, Prim. Dent. Care 8 (1) (2001) 5–11.
[4] T.M. Auschill, N.B. Arweiler, M. Brecx, E. Reich, A. Sculean, L. Netuschil, The effect of dental restorative materials on dental biofilm, Eur. J. Oral Sci. 110 (1) (2002) 48–53.
[5] A. Carlen, K. Nikdel, A. Wennerberg, K. Holmberg, J. Olsson, Surface characteristics and in vitro biofilm formation on glass ionomer and composite resin, Biomaterials 22 (5) (2001) 481–487.
[6] M. Quirynen, The clinical meaning of the surface roughness and the surface free energy of intra-oral hard substrata on the microbiology of the supra- and subgingival plaque: results of in vitro and in vivo experiments, J. Dent. 22 (Suppl. 1) (1994) S13–6.
[7] F.A. Scannapieco, Saliva-bacterium interactions in oral microbial ecology, Crit. Rev. Oral Biol. Med. 5 (3–4) (1994) 203–248.
[8] P. Senawongse, P. Pongprueksa, Surface roughness of nanofill and nanohybrid resin composites after polishing and brushing, J. Esthet. Restor. Dent. 19 (5) (2007) 265–273 discussion 74–5.
[9] H.B. Ahn, S.J. Ahn, S.J. Lee, T.W. Kim, D.S. Nahm, Analysis of surface roughness and surface free energy characteristics of various orthodontic materials, Am. J. Orthod. Dentofacial Orthop. 136 (5) (2009) 668–674.
[10] W. Weinmann, C. Thalacker, R. Guggenberger, Siloranes in dental composites, Dent. Mater. 21 (1) (2005) 68–74.
[11] W. Lien, K.S. Vandewalle, Physical properties of a new silorane-based restorative system, Dent. Mater. 26 (4) (2010) 337–344.
[12] S. Duarte Jr., A.C. Botta, J.H. Phark, A. Sadan, Selected mechanical and physical properties and clinical application of a new low-shrinkage composite restoration, Quintessence Int. 40 (8) (2009) 631–638.
[13] N. Ilie, R. Hickel, Macro-, micro- and nano-mechanical investigations on silorane and methacrylate-based composites, Dent. Mater. 25 (6) (2009) 810–819.
[14] H. Schweikl, G. Schmalz, W. Weinmann, Mutagenic activity of structurally related oxiranes and siloranes in Salmonella typhimurium, Mutat. Res. 521 (1–2) (2002) 19–27.
[15] K. Ikemura, F.R. Tay, Y. Kouro, T. Endo, M. Yoshiyama, K. Miyai, et al., Optimizing filler content in an adhesive system containing pre-reacted glass-ionomer fillers, Dent. Mater. 19 (2) (2003) 137–146.
[16] K. Ikemura, F.R. Tay, T. Endo, D.H. Pashley, A review of chemical-approach and ultramorphological studies on the development of fluoride-releasing dental adhesives comprising new pre-reacted glass ionomer (PRG) fillers, Dent. Mater. J. 27 (3) (2008) 315–339.
[17] M. Quirynen, C.M. Bollen, The influence of surface roughness and surface-free energy on supra- and subgingival plaque formation in man: a review of the literature, J. Clin. Periodontol. 22 (1) (1995) 1–14.
[18] W. Teughels, N. Van Assche, I. Sliepen, M. Quirynen, Effect of material characteristics and/or surface topography on biofilm development, Clin. Oral Implants Res. 17 (Suppl. 2) (2006) 68–81.
[19] M. Quirynen, C.M. Bollen, W. Papaioannou, J. Van Eldere, D. van Steenberghe, The influence of titanium abutment surface roughness on plaque accumulation and gingivitis: short-term observations, Int. J. Oral Maxillofac. Implants 11 (2) (1996) 169–178.
[20] C.M. Bollen, P. Lambrechts, M. Quirynen, Comparison of surface roughness of oral hard materials to the threshold surface roughness for bacterial plaque retention: a review of the literature, Dent. Mater. 13 (4) (1997) 258–269.
[21] F. Aykent, I. Yondem, A.G. Ozyesil, S.K. Gunal, M.C. Avunduk, S. Ozkan, Effect of different finishing techniques for restorative materials on surface roughness and bacterial adhesion, J. Prosthet. Dent. 103 (4) (2010) 221–227.
[22] S.P. Lee, S.J. Lee, B.S. Lim, S.J. Ahn, Surface characteristics of orthodontic materials and their effects on adhesion of mutans streptococci, Angle Orthod. 79 (2) (2009) 353–360.
[23] T. Lie, Ultrastructural study of early dental plaque formation, J. Periodontal Res. 13 (5) (1978) 391–409.
[24] T. Lie, Morphologic studies on dental plaque formation, Acta Odontol. Scand. 37 (2) (1979) 73–85.
[25] R. Buergers, W. Schneider-Brachert, S. Hahnel, M. Rosentritt, G. Handel, Streptococcal adhesion to novel low-shrink silorane-based restorative, Dent. Mater. 25 (2) (2009) 269–275.
[26] J.D. Eick, S.P. Kotha, C.C. Chappelow, K.V. Kilway, G.J. Giese, A.G. Glaros, et al., Properties of silorane-based dental resins and composites containing a stress-reducing monomer, Dent. Mater. 23 (8) (2007) 1011–1017.
[27] L. Mei, H.J. Busscher, H.C. van der Mei, Y. Chen, J. de Vries, Y. Ren, Oral bacterial adhesion forces to biomaterial surfaces constituting the bracket-adhesive-enamel junction in orthodontic treatment, Eur. J. Oral Sci. 117 (4) (2009) 419–426.
[28] J. Chandra, J.D. Patel, J. Li, G. Zhou, P.K. Mukherjee, T.S. McCormick, et al., Modification of surface properties of biomaterials influences the ability of Candida albicans to form biofilms, Appl. Environ. Microbiol. 71 (12) (2005) 8795–8801.
[29] S. Nomura, F. Lundberg, M. Stollenwerk, K. Nakamura, A. Ljungh, Adhesion of staphylococci to polymers with and without immobilized heparin in cerebrospinal fluid, J. Biomed. Mater. Res. 38 (1) (1997) 35–42.
[30] J.K. Baveja, M.D. Willcox, E.B. Hume, N. Kumar, R. Odell, L.A. Poole-Warren, Furanones as potential anti-bacterial coatings on biomaterials, Biomaterials 25 (20) (2004) 5003–5012.
[31] H. Tang, A. Wang, X. Liang, T. Cao, S.O. Salley, J.P. McAllister 3rd, et al., Effect of surface proteins on Staphylococcus epidermidis adhesion and colonization on silicone, Colloids Surf. B Biointerfaces 51 (1) (2006) 16–24.
[32] M. Gyo, T. Nikaido, K. Okada, J. Yamauchi, J. Tagami, K. Matin, Surface response of fluorine polymer-incorporated resin composites to cariogenic biofilm adherence, Appl. Environ. Microbiol. 74 (5) (2008) 1428–1435.
[33] J.T. Hirvi, T.A. Pakkanen, Enhanced hydrophobicity of rough polymer surfaces, J. Phys. Chem. B 111 (13) (2007) 3336–3341.
[34] H.J. Busscher, A.W.J. Van Pelt, P. De Boer, H.P. De Jong, J. Arends, The effect of surface roughening of polymers on measured contact angles of liquids, Colloids Surf. 9 (1984) 319–331.
[35] A. Ionescu, E. Wutscher, E. Brambilla, S. Schneider-Feyrer, F.J. Giessibl, S. Hahnel, Influence of surface properties of resin-based composites on in vitro Streptococcus mutans biofilm development, Eur. J. Oral Sci. 120 (5) (2012) 458–465.
[36] R. Burgers, W. Schneider-Brachert, M. Rosentritt, G. Handel, S. Hahnel, Candida albicans adhesion to composite resin materials, Clin. Oral Invest. 13 (3) (2009) 293–299.
[37] C. Pm, G. Rf, C. van Oss, Determination of the acid-base characteristics of clay mineral surfaces by contact angle measurements-implications for the adsorption of organic solutes from aqueous media, J. Adhes. Sci. Technol. 19 (4) (1990) 267–275.
[38] J. Satou, A. Fukunaga, N. Satou, H. Shintani, K. Okuda, Streptococcal adherence on various restorative materials, J. Dent. Res. 67 (3) (1988) 588–591.
[39] C.M. Bollen, W. Papaioanno, J. Van Eldere, E. Schepers, M. Quirynen, D. van Steenberghe, The influence of abutment surface roughness on plaque accumulation and peri-implant mucositis, Clin. Oral Implants Res. 7 (3) (1996) 201–211.
[40] A.A. Adamson, A.P. Gast, Physical Chmistry of Surfaces, Wiley-Interscience, New York, 1997, pp. 358.
[41] H. Nagem Filho, M.T. D'Azevedo, H.D. Nagem, F.P. Marsola, Surface roughness of composite resins after finishing and polishing, Braz. Dent. J. 14 (1) (2003) 37–41.
[42] Z. Ergucu, L.S. Turkun, Surface roughness of novel resin composites polished with one-step systems, Oper. Dent. 32 (2) (2007) 185–192.
[43] D. Sarac, Y.S. Sarac, S. Kulunk, C. Ural, T. Kulunk, The effect of polishing techniques on the surface roughness and color change of composite resins, J. Prosthet. Dent. 96 (1) (2006) 33–40.
[44] M. Baseren, Surface roughness of nanofill and nanohybrid composite resin and ormocer-based tooth-colored restorative materials after several finishing and polishing procedures, J. Biomater. Appl. 19 (2) (2004) 121–134.
[45] S. Joniot, J.P. Salomon, J. Dejou, G. Gregoire, Use of two surface analyzers to evaluate the surface roughness of four esthetic restorative materials after polishing, Oper. Dent. 31 (1) (2006) 39–46.
[46] P.O. Glantz, Adhesion to teeth, Int. Dent. J. 27 (4) (1977) 324–332.
[47] S.D. Heintze, M. Forjanic, K. Ohmiti, V. Rousson, Surface deterioration of dental materials after simulated toothbrushing in relation to brushing time and load, Dent. Mater. 26 (4) (2010) 306–319.
[48] A.H. Tjan, C.A. Chan, The polishability of posterior composites, J. Prosthet. Dent. 61 (2) (1989) 138–146.
[49] P. Berthold, Formation of salivary coating and dental plaque on two different supporting materials: an electron microscopic study, J. Periodontol. 50 (8) (1979) 397–405.
[50] G. Nakazato, H. Tsuchiya, M. Sato, M. Yamauchi, In vivo plaque formation on implant materials, Int. J. Oral Maxillofac. Implants 4 (4) (1989) 321–326.
[51] N.P. Boks, W. Norde, H.C. van der Mei, H.J. Busscher, Forces involved in bacterial adhesion to hydrophilic and hydrophobic surfaces, Microbiology 154 (Pt. 10) (2008) 3122–3133.
[52] S. Hahnel, A. Henrich, M. Rosentritt, G. Handel, R. Burgers, Influence of artificial ageing on surface properties and Streptococcus mutans adhesion to dental composite materials, J. Mater. Sci. Mater. Med. 21 (2) (2010) 823–833.
[53] E.A. Vogler, Structure and reactivity of water at biomaterial surfaces, Adv. Colloid. Interface Sci. 74 (1998) 69–117.
[54] Y.H. An, R.J. Friedman, Concise review of mechanisms of bacterial adhesion to biomaterial surfaces, J Biomed. Mater. Res. 43 (3) (1998) 338–348.
[55] S. Hahnel, M. Rosentritt, G. Handel, R. Burgers, Influence of saliva substitute films on initial Streptococcus mutans adhesion to enamel and dental substrata, J. Dent. 36 (12) (2008) 977–983.
[56] J. Satou, A. Fukunaga, A. Morikawa, I. Matsumae, N. Satou, H. Shintani, Streptococcal adherence to uncoated and saliva-coated restoratives, J. Oral Rehabil. 18 (5) (1991) 421–429.
[57] C.E. Christersson, L. Lindh, T. Arnebrant, Film-forming properties and viscosities of saliva substitutes and human whole saliva, Eur. J. Oral Sci. 108 (5) (2000) 418–425.
[58] I.H. Pratt-Terpstra, A.H. Weerkamp, H.J. Busscher, Adhesion of oral streptococci from a flowing suspension to uncoated and albumin-coated surfaces, J. Gen. Microbiol. 133 (11) (1987) 3199–3206.